INTERNATIONAL JOURNAL FOR NUMERICAL METHODS IN FLUIDS
Int. J. Numer. Meth. Fluids 2007; **55**:483–507
Published online 20 March 2007 in Wiley InterScience (www.interscience.wiley.com). DOI: 10.1002/fld.1479

Efficient high-resolution relaxation schemes for hyperbolic systems of conservation laws

Ritesh Kumar*, † and M. K. Kadalbajoo

Department of Mathematics and Statistics, Indian Institute of Technology Kanpur, Kanpur 208016, India

SUMMARY

In this work, we present a total variation diminishing (TVD) scheme in the zero relaxation limit for nonlinear hyperbolic conservation law using flux limiters within the framework of a relaxation system that converts a nonlinear conservation law into a system of linear convection equations with nonlinear source terms. We construct a numerical flux for space discretization of the obtained relaxation system and modify the definition of the smoothness parameter depending on the direction of the flow so that the scheme obeys the physical property of hyperbolicity. The advantages of the proposed scheme are that it can give second-order accuracy everywhere without introducing oscillations for 1-D problems (at least with) smooth initial condition. Also, the proposed scheme is more efficient as it works for any non-zero constant value of the flux limiter $\phi \in [0, 1]$, where other TVD schemes fail. The resulting scheme is shown to be TVD in the zero relaxation limit for 1-D scalar equations. Bound for the limiter function is obtained. Numerical results support the theoretical results. Copyright © 2007 John Wiley & Sons, Ltd.

Received 26 May 2006; Revised 6 February 2007; Accepted 8 February 2007

KEY WORDS: conservation laws; high-resolution schemes; total variation diminishing schemes; relaxation methods

1. INTRODUCTION

Consider the 1-D system of conservation laws

$$\frac{\partial \mathbf{u}}{\partial t} + \frac{\partial \mathbf{f}(\mathbf{u})}{\partial x} = 0 \qquad \mathbf{u}(x, 0) = \mathbf{u}_0(x), \quad x \in \mathbb{R} \tag{1}$$

together with appropriate boundary conditions, where $\mathbf{u} \in \mathbb{R}^m$ and the flux function $\mathbf{f}(\mathbf{u}) : \mathbb{R}^m \to \mathbb{R}^m$ is nonlinear. It is seen that the classical first-order difference methods for (1) are monotone and

*Correspondence to: Ritesh Kumar, Department of Mathematics and Statistics, Indian Institute of Technology Kanpur, Kanpur 208016, India.
†E-mail: riteshkd@gmail.com

Copyright © 2007 John Wiley & Sons, Ltd.

stable, but suffer from numerical dissipation and make the solution get smeared out and are often grossly inaccurate. On the other hand, classical higher-order numerical schemes are less dissipative but are susceptible to numerical instabilities and exhibit spurious oscillations around the point of discontinuity called the sonic or extreme points, or in the region of steep gradients. In fact, even if the initial condition for (1) is very smooth, spurious oscillations get introduced by the higher-order schemes. Apart from the numerical instabilities, fundamental mechanical or thermodynamical principles can be violated [1–7].

In recent years, efforts have been made to build schemes which can give accuracy of high order as well as avoid spurious oscillations. In order to do so, a class of high-resolution schemes, known as total variation diminishing (TVD) schemes, was proposed in [8]. Such high-resolution schemes are conservative, generally (at most places) second-order accurate, non-oscillatory in nature and capable of resolving discontinuity in the solution. The basic idea of constructing TVD schemes is to use a linear combination of a low-order scheme and a high-order accurate scheme using a limiter function. This class of schemes give second-order accuracy in the smooth region of solution and first-order accuracy in the region of steep gradient or around sonic points. *It has been observed in the literature that maintaining high-order accuracy at extreme points is impossible with TVD schemes* (e.g. see [5, p. 177]). In fact Osher and Chakravarthy considered the 'semi-discrete' class of TVD schemes and showed that they are at most first-order accurate at non-sonic critical points of the solution [9]. In this work, we propose a relaxation scheme for system of conservation laws. It is a TVD scheme that can be second-order accurate even at the sonic points. To construct the relaxation scheme, we extend the numerical flux functions proposed in our previous work [10, 11] for nonlinear conservation laws using the framework of relaxation method proposed in [12]. It reduces the nonlinear conservation law into a system of linear convection equations with a nonlinear source term.

Apply the relaxation method to problem (1) to obtain a relaxation system of the form

$$\frac{\partial \mathbf{u}}{\partial t} + \frac{\partial \mathbf{v}}{\partial x} = 0$$

$$\frac{\partial \mathbf{v}}{\partial t} + \mathbf{A}^2 \frac{\partial \mathbf{u}}{\partial x} = -\frac{1}{\varepsilon}(\mathbf{v} - \mathbf{f}(\mathbf{u})), \quad \varepsilon > 0 \tag{2}$$

$$\mathbf{u}(x, 0) = \mathbf{u}_0(x), \quad \mathbf{v}(x, 0) = \mathbf{f}(\mathbf{u}_0(x))$$

where $\mathbf{v} \in \mathbb{R}^m$, $\mathbf{A}^2 = \text{diag}(a_1^2, \ldots, a_m^2) \in \mathbb{R}^m$ and ε is the relaxation rate. For ε sufficiently small, one can obtain good approximation to the original conservation laws (1) by solving (2). For $\varepsilon \ll 1$ such relaxation system is called stiff relaxation system. A good numerical discretization of (2) should possess a discrete analogy of the continuous zero relaxation limit, in the sense that the zero relaxation limit ($\varepsilon \to 0$ for fixed mesh size) of the numerical discretization should be consistent and stable discretization to (1). The semi-discrete numerical schemes for hyperbolic conservation laws share the same relaxation limit as that of (1). The relaxation system (2) has a typical semi-linear structure with $2m$ linear characteristic variables, $\mathbf{v} \pm \mathbf{Au}$, that travel with the *frozen* characteristic speeds $\pm \mathbf{A}$, respectively. The numerical approximation will be applied to $\mathbf{v} \pm \mathbf{Au}$. Thus, the relaxation method replaces a nonlinear system into a semi-linear system with the main advantage that it can be solved numerically without introducing computationally costly Riemann solvers. Note that every characteristic value λ of $\mathbf{f}'(\mathbf{u})$ interlace with those $\pm a_i$, $i = 1 \ldots m$ of the

Copyright © 2007 John Wiley & Sons, Ltd.

DOI: 10.1002/fld

relaxation system (2) by

$$\frac{|\lambda|}{a_i} \leqslant 1, \quad i = 1 \ldots m, \ \ \forall \lambda \tag{3}$$

This condition is called sub-characteristic condition, given by Liu [13].

In the small relaxation limit $\varepsilon \to 0^+$, the relaxation system can be approximated to leading order by

$$\mathbf{v} = \mathbf{f}(\mathbf{u}) \tag{4}$$

$$\frac{\partial}{\partial t}\mathbf{u} + \frac{\partial}{\partial x}\mathbf{f}(\mathbf{u}) = 0 \tag{5}$$

the state satisfying (4) is called the local equilibrium and (5) is the original conservation law (1).

The relaxation system as defined above was first given in [12] in which, following the method of lines, a first-order upwind scheme along with first-order implicit Runge–Kutta scheme and a second-order MUSCL scheme along with the second-order implicit-explicit (IMEX) Runge–Kutta method for space and for time integration were used.

In this paper we follow the same idea and give an efficient relaxation scheme by extending the numerical flux function in [10] for relaxation system (2). The derivation of the scheme is presented. We define the smoothness parameter such that the resulting scheme respects the physical hyperbolicity condition. The second-order accurate relaxation scheme is shown to be TVD in the zero relaxation limit. The proposed scheme is efficient and by fixing flux limiter function to unity, one can have a second-order accurate TVD relaxation scheme. Extension of the scheme for 2-D case is given. Numerical test results and discussion for some nonlinear hyperbolic conservation laws followed by conclusion is presented at last.

2. RELAXATION SCHEMES

In this section we give the basic ideas of relaxation schemes. Special attention is paid to the second-order MUSCL relaxation scheme given in [12]. Relaxation schemes are, in fact, a combination of non-oscillatory space discretization and an IMEX time integration of resulting semi-discrete system. The fully discrete system of (2) is called the relaxing scheme while that of the limiting system, as the relaxation rate tends to zero ($\varepsilon \to 0$), is called the relaxed scheme. For clarity of approach, we assume, an equally spaced grid $\Delta x := x_{i+1/2} - x_{i-1/2}$ and a uniform time step $\Delta t := t_{n+1} - t_n$ to discretize the system (2). We use the notation

$$\omega^n_{i+1/2} = \omega(x_{i+1/2}, t_n) \quad \text{and} \quad \omega^n_i = \frac{1}{\Delta x}\int_{x_{i-1/2}}^{x_{i+1/2}} \omega(x, t_n)\, \mathrm{d}x$$

to denote the point-value and the approximate cell-average of the function ω over $x = x_{i-1/2}$, $t = t_n$; and $x = x_{i+1/2}$, $t = t_n$. Now define,

$$D_x \omega_i := \frac{\omega_{i+1/2} - \omega_{i-1/2}}{\Delta x} \tag{6}$$

Copyright © 2007 John Wiley & Sons, Ltd.

DOI: 10.1002/fld

A semi-discrete approximation for the system of Equation (2), using the method of lines, can be written as

$$\begin{aligned} \frac{\mathrm{d}\mathbf{u_i}}{\mathrm{d}t} + D_x \mathbf{v_i} &= 0 \\ \frac{\mathrm{d}\mathbf{v_i}}{\mathrm{d}t} + \mathbf{A}^2 D_x \mathbf{u_i} &= -\frac{1}{\varepsilon}(\mathbf{v_i} - \mathbf{f}(\mathbf{u_i})) \end{aligned} \tag{7}$$

Note that space and time discretization here are treated separately. Any such approximation for the numerical flux in (6) should be accompanied by an ODE solver for (7) of the same accuracy. We present the second-order relaxing scheme of [12] as follows.

In the construction of second-order scheme, MUSCL method [14] for the discretization of the characteristic variables $\mathbf{v} \pm \mathbf{Au}$ was used. This method yields the semi-discrete system (7), where the numerical fluxes for the pth component of (7) are,

$$\begin{aligned} u_{i+1/2} &= \frac{u_i + u_{i+1}}{2} - \frac{v_{i+1} - v_i}{2a_p} + \frac{\sigma_i^+ + \sigma_{i+1}^-}{4a_p} \\ v_{i+1/2} &= \frac{v_i + v_{i+1}}{2} - a_p \frac{u_{i+1} - u_i}{2} + \frac{\sigma_i^+ - \sigma_{i+1}^-}{4} \end{aligned} \tag{8}$$

where the slopes of pth component of characteristic variables $\mathbf{v} \pm \mathbf{Au}$ i.e. $v \pm a_p u$ are defined as

$$\begin{aligned} \sigma_i^{\pm} &= \Delta_+(v_i \pm a_p u_i)\phi(\theta_i^{\pm}) \\ \theta_i^{\pm} &= \frac{\Delta_-(v_i \pm a_p u_i)}{\Delta_+(v_i \pm a_p u_i)} \end{aligned} \tag{9}$$

with $\Delta_- u_{i+1} = \Delta_+ u_i = \Delta u_{i+1/2} = u_{i+1} - u_i$.

Here, ϕ is the slope limiter function and θ is the smoothness parameter which is the ratio of consecutive difference of the characteristic variable. The chosen slope limiter is the so-called min-mod limiter

$$\phi(\theta) = \max(0, \min(1, \theta)) \tag{10}$$

and sharper van Leer limiter,

$$\phi(\theta) = \frac{|\theta| + \theta}{1 + |\theta|} \tag{11}$$

Note that, one can obtain the first-order scheme presented in [12] by putting $\sigma = 0$ or $\phi = 0$, in (8) and (9). A second-order IMEX Runge–Kutta scheme [15] for hyperbolic conservation laws with stiff relaxation terms was used to integrate (7) in time. Table I shows its corresponding Butcher tables, where the left and right tables represent the explicit and implicit Runge–Kutta schemes, respectively.

Table I. Butcher table.

0	0	0	−1	−1	0
1	1	0	2	1	1
	1/2	1/2		1/2	1/2

Copyright © 2007 John Wiley & Sons, Ltd.

DOI: 10.1002/fld

3. CONSTRUCTION OF PROPOSED SECOND-ORDER RELAXATION SCHEME

In this section we construct a numerical flux function for the relaxation system (2). We modify definition (9) of the smoothness parameter θ in such a way that the resulting numerical flux functions respect the physical hyperbolicity property of hyperbolic conservation laws.

Consider the scalar equation

$$u_t + au_x = 0 \tag{12}$$

To construct a high-resolution scheme we define the numerical flux function of the new scheme in terms of numerical flux functions of the first-order upwind scheme (h_L) and second-order upwind scheme (h_H) as

$$h^n_{i+1/2} = h^n_{L_{i+1/2}} + \phi^{\pm}_i [h^n_{H_{i+1/2}} - h^n_{L_{i+1/2}}] \tag{13}$$

where h_L and h_H are the numerical flux functions of first-order and second-order upwind schemes, respectively, and are given by

$$h^n_{L_{i+1/2}} = \begin{cases} au^n_i, & a>0 \\ au^n_{i+1}, & a<0 \end{cases} \tag{14}$$

$$h^n_{H_{i+1/2}} = \begin{cases} \dfrac{a}{2}(3u^n_i - u^n_{i-1}), & a>0 \\ \dfrac{a}{2}(3u^n_{i+1} - u^n_{i+2}), & a<0 \end{cases} \tag{15}$$

Here, ϕ is some function of consecutive differences, i.e. $\phi^{\pm}_i = \phi(\theta^{\pm}_i)$. ϕ and $\theta^{\pm}$ (both yet to be defined) are called the flux limiter function and the smoothness parameter, respectively. One need to define ϕ in such a way that the resulting numerical flux function has the smoothing capabilities of the lower-order scheme when it is necessary (i.e. near discontinuities) and the accuracy of the higher-order scheme when it is possible (i.e. in the smooth sections of solution). Note that, the general numerical flux function of high-resolution scheme for this linear problem (dropping out superscript for nth time level) can be written as

$$h_{i+1/2} = \begin{cases} au_i + \dfrac{a}{2}\phi^+_i(u_i - u_{i-1}), & a>0 \\ au_{i+1} - \dfrac{a}{2}\phi^-_{i+1}(u_{i+2} - u_{i+1}), & a<0 \end{cases}$$

Now depending on the direction of flow we modify the definition of the smoothness parameter as

$$\phi^{\pm}_i = \phi(\theta^{\pm}_i) \quad \text{with } \theta^{\pm}_i = \frac{\Delta_{\mp} u_{i-1}}{\Delta_{\mp} u_i}$$

$\theta^{\pm}_i$ is geometrically shown in Figure 1.

Copyright © 2007 John Wiley & Sons, Ltd.

DOI: 10.1002/fld

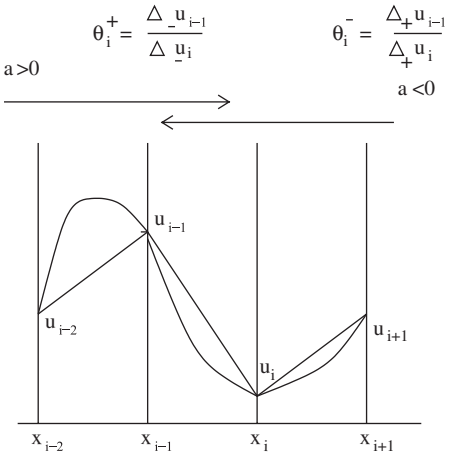

Figure 1. Smoothness parameter.

Extending the numerical flux function for the pth component of characteristic variables $(v \pm a_p u)$ associated with the linear relaxation system (2), we have

$$(v + a_p u)_{i+1/2} = v_i + a_p u_i + \frac{\phi(\theta_i^+)}{2}(v_i - v_{i-1} + a_p(u_i - u_{i-1})) \tag{16}$$

$$(v - a_p u)_{i+1/2} = v_{i+1} - a_p u_{i+1} - \frac{\phi(\theta_{i+1}^-)}{2}(v_{i+2} - v_{i+1} - a_p(u_{i+2} - u_{i+1})) \tag{17}$$

solving (16) and (17) one can get

$$\begin{aligned} u_{i+1/2} &= \frac{1}{2}(u_{i+1} + u_i) - \frac{1}{2a_p}(v_{i+1} - v_i) + \frac{1}{4a_p}(\sigma_i^+ + \sigma_{i+1}^-) \\ v_{i+1/2} &= \frac{1}{2}(v_{i+1} + v_i) - \frac{a_p}{2}(u_{i+1} - u_i) + \frac{1}{4}(\sigma_i^+ - \sigma_{i+1}^-) \end{aligned} \tag{18}$$

where slopes are defined as

$$\sigma_i^{\pm} = \Delta_{\mp}(v_i \pm a_p u_i)\phi(\theta_i^{\pm}) \tag{19}$$

and depending on the direction of flow, we define the smoothness parameter for the characteristic variable $(v \pm a_p u)$ as

$$\theta_i^+ = \frac{\Delta_-(v_{i-1} + a_p u_{i-1})}{\Delta_-(v_i + a_p u_i)}, \quad \theta^- = \frac{\Delta_+(v_{i-1} - a_p u_{i-1})}{\Delta_+(v_i - a_p u_i)} \tag{20}$$

In order to integrate in time we use the same second-order IMEX Runge–Kutta scheme given in Table I. Consequently, we can formulate the second-order relaxation scheme to integrate (2)

Copyright © 2007 John Wiley & Sons, Ltd.

DOI: 10.1002/fld

as follows:

Given $\{\mathbf{u_i^n}, \mathbf{v_i^n}\}$, $\{\mathbf{u_i^{n+1}}, \mathbf{v_i^{n+1}}\}$ are computed by

$$\begin{aligned}
\mathbf{u}_i^* &= \mathbf{u}_i^n \\
\mathbf{v}_i^* &= \mathbf{v}_i^n + \frac{\Delta t}{\varepsilon}(\mathbf{v}_i^* - \mathbf{f}(\mathbf{u}_i^*)) \\
\mathbf{u}_i^{(1)} &= \mathbf{u}_i^* - \Delta t D_x \mathbf{v}_i^* \\
\mathbf{v}_i^{(1)} &= \mathbf{v}_i^* - \Delta t \mathbf{A}^2 D_x \mathbf{u}_i^* \\
\mathbf{u}_i^{**} &= \mathbf{u}_i^{(1)} \\
\mathbf{v}_i^{**} &= \mathbf{v}_i^{(1)} - \frac{\Delta t}{\varepsilon}(\mathbf{v}_i^{**} - \mathbf{f}(\mathbf{u}_i^{**})) - \frac{2\Delta t}{\varepsilon}(\mathbf{v}_i^* - \mathbf{f}(\mathbf{u}_i^*)) \\
\mathbf{u}_i^{(2)} &= \mathbf{u}_i^{**} - \Delta t D_x \mathbf{v}_i^{**} \\
\mathbf{v}_i^{(2)} &= \mathbf{v}_i^{**} - \Delta t \mathbf{A}^2 D_x \mathbf{u}_i^{**} \\
\mathbf{u}_i^{n+1} &= \tfrac{1}{2}(\mathbf{u}_i^n + \mathbf{u}_i^{(2)}) \\
\mathbf{v}_i^{n+1} &= \tfrac{1}{2}(\mathbf{v}_i^n + \mathbf{v}_i^{(2)})
\end{aligned} \tag{21}$$

It was shown in [12] that the variables $\mathbf{v}_i^*$ and $\mathbf{v}_i^{**}$ approximate the local equilibrium $\mathbf{f}(\mathbf{u}_i^*)$ and $\mathbf{f}(\mathbf{u}_i^{**})$, respectively, when $\varepsilon \to 0$. Hence, relaxed system can be obtained by passing $\varepsilon \to 0$, and is given as

$$\frac{\partial}{\partial t}\mathbf{u} + \frac{\partial}{\partial x}\mathbf{f}(\mathbf{u}) = 0 \tag{22}$$

Its corresponding relaxed scheme is given by its semi-discrete conservative approximation

$$\frac{\partial}{\partial t}\mathbf{u}_i + \frac{1}{\Delta x}(\mathbf{F}_{i+1/2} - \mathbf{F}_{i-1/2}) = 0 \tag{23}$$

where the pth component of the numerical flux $\mathbf{F}$ is

$$\begin{aligned}
F_{i+1/2}^p &= v_{i+1/2}|_{v=f^p(\mathbf{u})} \\
&= \frac{1}{2}(f^p(\mathbf{u}_{i+1}) + f^p(\mathbf{u}_i)) - \frac{a_p}{2}(u_{i+1} - u_i) + \frac{1}{4}(\sigma_i^+ - \sigma_{i+1}^-)\Big|_{v=f^p(\mathbf{u})}
\end{aligned} \tag{24}$$

with the slope limiters

$$\begin{aligned}
\sigma_i^{\pm}|_{v=f^p(\mathbf{u})} &= \Delta_{\mp}(f^p(u_i) \pm a_p u_i)\phi(\theta_i^{\pm}) \\
\theta_i^{\pm} &= \frac{\Delta_{\mp}(f^p(\mathbf{u}_{i-1}) \pm a_p u_{i-1})}{\Delta_{\mp}(f^p(\mathbf{u}_i) \pm a_p u_i)}
\end{aligned} \tag{25}$$

Copyright © 2007 John Wiley & Sons, Ltd.

DOI: 10.1002/fld

Consequently, a second-order relaxed scheme is obtained, based on the left explicit Table I, as

$$\begin{aligned}
\mathbf{u}_i^{(1)} &= \mathbf{u}_i^n - \Delta t\, D_x \mathbf{v}_i^n|_{\mathbf{v}_i^n = \mathbf{f}(\mathbf{u}_i^n)} \\
\mathbf{u}_i^{(2)} &= \mathbf{u}_i^{(1)} - \Delta t\, D_x \mathbf{v}_i^{(1)}|_{\mathbf{v}_i^{(1)} = \mathbf{f}(\mathbf{u}_i^{(1)})} \\
\mathbf{u}_i^{n+1} &= \tfrac{1}{2}(\mathbf{u}_i^n + \mathbf{u}_i^{(2)})
\end{aligned} \tag{26}$$

One can see from (24) and (25) that $F^p(u, \ldots, u) = f^p(u)$, where F^p and f^p are the pth components of $\mathbf{F}$ and $\mathbf{f}$. Hence, from the definition of consistent approximation, the second-order discretization using numerical flux function (24) and (25) is consistent to (22).

Note that the time discretization, in the limit when $\varepsilon \to 0$, converges to (26). This second-order TVD Runge–Kutta method is given by Shu [16], and is also referred to as strong stability-preserving (SSP) time discretization [17].

Also note that using these schemes neither algebraic equations nor nonlinear source terms can arise. In addition, the second-order relaxation schemes are stable and independent of ε, so the choice of Δt is based on usual Courant–Friedrichs–Lewy (CFL) condition, $C \leqslant \frac{1}{2}$, (as it is the CFL condition for second-order accurate conservative scheme obtained by using numerical flux function defined in (15)), i.e.

$$C = \max_{1 \leqslant k \leqslant m} a_k^2 \frac{\Delta t}{\Delta x} \leqslant \frac{1}{2} \tag{27}$$

4. TVD ANALYSIS OF THE RELAXED SCHEME

For sufficiently small ε, the leading behaviour of the relaxation scheme is governed by the relaxed scheme. Hence, it is important to study the behaviour of the relaxed scheme. In this section we give the conditions on the flux limiter function ϕ so that, the resulting relaxed scheme for 1-D scalar conservation law is TVD. Consider the 1-D scalar conservation law

$$\frac{\partial}{\partial t} u + \frac{\partial}{\partial x} g(u) = 0, \quad (x, t) \in \mathbb{R}^1 \times \mathbb{R}_+, \quad u \in \mathbb{R}^1 \tag{28}$$

with initial data $u(x, 0) = u_0(x)$. Its corresponding relaxation system following (2) is

$$\begin{aligned}
&\frac{\partial}{\partial t} u + \frac{\partial}{\partial x} v = 0, \quad v \in \mathbb{R}^1 \\
&\frac{\partial}{\partial t} v + a^2 \frac{\partial}{\partial x} u = -\frac{1}{\varepsilon}(v - g(u))
\end{aligned} \tag{29}$$

where a is a positive constant satisfying the sub-characteristic condition

$$-a \leqslant g'(u) \leqslant a \quad \forall u \tag{30}$$

Copyright © 2007 John Wiley & Sons, Ltd.

DOI: 10.1002/fld

The one-step conservative scheme for the relaxation system (29), with uniform grid is given by

$$\begin{aligned}
&\frac{1}{\Delta t}(u_i^{n+1}-u_i^n)+\frac{1}{\Delta x}(v_{i+1/2}^n-v_{i-1/2}^n)=0\\
&\frac{1}{\Delta t}(v_i^{n+1}-v_i^n)+\frac{a^2}{\Delta x}(u_{i+1/2}^n-u_{i-1/2}^n)=-\frac{1}{\varepsilon}(v_i^{n+1}-g(u_i^{n+1}))
\end{aligned} \tag{31}$$

Using the numerical flux function (18), the second-order relaxation scheme for the relaxation system (2) is obtained. Rewriting the numerical flux function (18) as

$$\begin{aligned}
u_{i+1/2}&=\frac{u_{i+1}+u_i}{2}-\frac{(v_{i+1}-v_i)}{2a}+\frac{\Delta x(1-\beta)}{4a}(\sigma_i^+ +\sigma_{i+1}^-)\\
v_{i+1/2}&=\frac{1}{2}(v_{i+1}+v_i)-\frac{a}{2}(u_{i+1}-u_i)+\frac{\Delta x(1-\beta)}{4}(\sigma_i^+ -\sigma_{i+1}^-)
\end{aligned} \tag{32}$$

where slopes are defined as

$$\begin{aligned}
\sigma_i^{\pm}&=\frac{1}{\Delta x}\Delta_{\mp}(v_i\pm au_i)\phi(\theta_i^{\pm})\\
\theta_i^{\pm}&=\frac{\Delta_{\mp}(v_{i-1}\pm au_{i-1})}{\Delta_{\mp}(v_i\pm au_i)}
\end{aligned} \tag{33}$$

and β is a positive constant such that,

$$\beta=\begin{cases} a\lambda\equiv C & \text{for forward Euler time discretization}\\ 0 & \text{for method of lines}\end{cases} \tag{34}$$

where $\lambda=\Delta t/\Delta x$.

Consider the case of forward Euler time discretization i.e. $\beta=c$ (for method of lines, similar analysis works). Dropping the superscript n for all quantities at time $t=t_n$, the corresponding relaxed scheme takes the form,

$$\begin{aligned}
v_i&=g(u_i)\\
\frac{u_i^{n+1}-u_i}{\Delta t}&=-\frac{1}{2\Delta x}(v_{i+1}-v_{i-1})+\frac{a}{2\Delta x}(u_{i+1}-2u_i+u_{i-1})\\
&\quad+\frac{(1-\beta)}{4}(\sigma_i^+-\sigma_{i+1}^--\sigma_{i-1}^++\sigma_i^-)
\end{aligned} \tag{35}$$

Recall that, a difference scheme is said to be a TVD scheme if the numerical solution obtained by the scheme satisfies

$$\sum_{k=-\infty}^{\infty}|\Delta_+u_k^{n+1}|\leqslant\sum_{k=-\infty}^{\infty}|\Delta_+u_k^n|\quad\forall n\geqslant 0 \tag{36}$$

Copyright © 2007 John Wiley & Sons, Ltd.

DOI: 10.1002/fld

Define

$$P_i = \frac{\lambda}{2}\left(a + \frac{g(u_{i+1}) - g(u_i)}{u_{i+1} - u_i}\right)$$
$$Q_i = \frac{\lambda}{2}\left(a - \frac{g(u_{i+1}) - g(u_i)}{u_{i+1} - u_i}\right) \tag{37}$$

Obviously, P_i and Q_i both are positive due to the sub-characteristic condition (30), i.e. $-a \leqslant g'(u) \leqslant a$. Using $v = g(u)$ and (37), one can write (35) as

$$u_i^{n+1} = u_i^n - P_{i-1}(u_i - u_{i-1}) + Q_i(u_{i+1} - u_i) + \frac{\Delta t}{4}(1-\beta)(\sigma_i^+ - \sigma_{i+1}^- - \sigma_{i-1}^+ + \sigma_i^-) \tag{38}$$

It directly follows from (38) that

$$u_{i+1}^{n+1} - u_i^{n+1} = (1 - P_i - Q_i)(u_{i+1} - u_i) + P_{i-1}(u_i - u_{i-1}) + Q_{i+1}(u_{i+2} - u_{i+1}) + R_{i+1/2} \tag{39}$$

where

$$R_{i+1/2} = \frac{\Delta t(1-\beta)}{4}(\sigma_{i+1}^+ - 2\sigma_i^+ + \sigma_{i-1}^+ - \sigma_{i+2}^- + 2\sigma_{i+1}^- - \sigma_i^-) \tag{40}$$

Now from the definition of slopes (33)

$$\sigma_i^+ = \frac{2}{\lambda \Delta x} P_{i-1}\phi(\theta_i^+)(u_i - u_{i-1})$$
$$\sigma_i^- = -\frac{2}{\lambda \Delta x} Q_i \phi(\theta_i^-)(u_{i+1} - u_i) \tag{41}$$

Using (41) in (40) and notation $\phi_i^\pm$ for $\phi(\theta_i^\pm)$, one can obtain

$$R_{i+1/2} = \tfrac{1}{2}(1-\beta)[(P_i\phi_{i+1}^+ + Q_i\phi_i^-)(u_{i+1} - u_i) + Q_{i+2}\phi_{i+2}^-(u_{i+3} - u_{i+2}) - 2Q_{i+1}\phi_{i+1}^-(u_{i+2} - u_{i+1}) - 2P_{i-1}\phi_i^+(u_i - u_{i-1}) + P_{i-2}\phi_{i-1}^+(u_{i-1} - u_{i-2})] \tag{42}$$

Using (42) in (39) yields

$$u_{i+1}^{n+1} - u_i^{n+1} = (1 - P_i - Q_i + \tfrac{1}{2}(1-\beta)[P_i\phi_{i+1}^+ + Q_i\phi_i^-](u_{i+1} - u_i) + [1-(1-\beta)\phi_i^+]P_{i-1}(u_i - u_{i-1}) + [1-(1-\beta)\phi_{i+1}^-]Q_{i+1}(u_{i+2} - u_{i+1}) + \tfrac{1}{2}(1-\beta)[P_{i-2}\phi_{i-1}^+(u_{i-1} - u_{i-2}) + Q_{i+2}\phi_{i+2}^-(u_{i+3} - u_{i+2})] \tag{43}$$

From (37) and the condition $0 \leqslant a\lambda \leqslant \frac{1}{2}$, one can deduce, $0 \leqslant P_i$, $Q_i \leqslant 1$ and $0 \leqslant P_i + Q_i \leqslant 1$, $\forall i$.

Copyright © 2007 John Wiley & Sons, Ltd.

DOI: 10.1002/fld

If the limiter function satisfies the condition, $0 \leqslant \phi \leqslant 1$ then, $(1-(P_i+Q_i)+\frac{1}{2}(1-\beta)\phi^+_{i+1}P_i+\frac{1}{2}(1-\beta)\phi^-_i Q_i) \geqslant 1-(P_i+Q_i) \geqslant 0$. Hence, all the coefficients on the right-hand side of (43) are non-negative. Taking modulus of both sides of (43)

$$\begin{aligned}|u^{n+1}_{i+1}-u^{n+1}_i| \leqslant{}& (1-(P_i+Q_i)+\tfrac{1}{2}(1-\beta)\phi^+_{i+1}P_i+\tfrac{1}{2}(1-\beta)\phi^-_i Q_i)|u_{i+1}-u_i| \\ &+[1-(1-\beta)\phi^+_i]P_{i-1}|u_i-u_{i-1}|+\tfrac{1}{2}(1-\beta)\phi^+_{i-1}P_{i-2}|u_{i-1}-u_{i-2}| \\ &+\tfrac{1}{2}(1-\beta)\phi^-_{i+2}Q_{i+2}|u_{i+3}-u_{i+2}| \\ &+(1-(1-\beta)\phi^-_{i+1}Q_{i+1})|u_{i+2}-u_{i+1}| \end{aligned} \tag{44}$$

Summing up over all i and adjusting the subscript in each term we get the desired result

$$\sum_{i=-\infty}^{\infty}|u^{n+1}_{i+1}-u^{n+1}_i| \leqslant \sum_{i=-\infty}^{\infty}|u^n_{i+1}-u^n_i| \quad \forall n \geqslant 0 \tag{45}$$

i.e.

$$TV(u^{n+1}) \leqslant TV(u^n)$$

We summarize the above analysis by using the following theorem.

Theorem

If the flux limiter function ϕ satisfies the condition $0 \leqslant \phi \leqslant 1$, then the relaxed scheme (39) is TVD provided that the sub-characteristic condition (30) and the CFL condition $0 \leqslant C \leqslant \frac{1}{2}$ is satisfied.

Remarks

1. The consistency and the TVD property of the proposed scheme implies that it is convergent, and converges to the physically correct weak solution of the original conservation law (1) (see [5]).
2. Note that, for any constant values of $\phi(\theta) \in [0, 1]$, $\forall\theta$, the resulting scheme is TVD. For $\phi = 0$, we have first-order accurate TVD scheme whereas $\phi = 1$ results into second-order accurate TVD scheme, hence one can get second-order accuracy, even at sonic points.
3. Note that in the existing TVD schemes using flux limiters [9, 12, 18], etc., the bounds on the flux limiter function are dependent on θ in order to make them TVD. Hence, one has to choose the limiter function in terms of θ and existing limiters e.g. min-mod, van Leer, etc., are designed to give $\phi = 0$ at extreme point where $\theta < 0$ to avoid the increase in total variation. Thus, the order of accuracy of these TVD schemes reduce to one at extreme points. On the other hand, in the proposed scheme, the bound on the limiter function ϕ is independent of the smoothness parameter θ. So one can choose any fixed value of ϕ in [0, 1] independent of θ. Hence, choosing $\phi = 1$ results into a second-order accurate relaxation scheme.

5. EXTENSION TO MULTIDIMENSIONAL PROBLEMS

Let us consider the 2-D hyperbolic system of conservation laws

$$\frac{\partial}{\partial t}\mathbf{u}+\frac{\partial}{\partial x}\mathbf{f}(\mathbf{u})+\frac{\partial}{\partial y}\mathbf{l}(\mathbf{u})=0, \quad (x, y) \in \mathbb{R}^2, \quad t>0 \tag{46}$$

Copyright © 2007 John Wiley & Sons, Ltd.

DOI: 10.1002/fld

where $\mathbf{f}(\mathbf{u})$ and $\mathbf{l}(\mathbf{u}) \in \mathbb{R}^2$ and are nonlinear functions, $\mathbf{u} \in \mathbb{R}^2$. Consider its corresponding relaxation system

$$\begin{aligned} &\frac{\partial \mathbf{u}}{\partial t} + \frac{\partial \mathbf{v}}{\partial x} + \frac{\partial \mathbf{w}}{\partial y} = 0 \\ &\frac{\partial \mathbf{v}}{\partial t} + \mathbf{A}^2 \frac{\partial \mathbf{u}}{\partial x} = -\frac{1}{\varepsilon}(\mathbf{v} - \mathbf{f}(\mathbf{u})) \\ &\frac{\partial \mathbf{w}}{\partial t} + \mathbf{B}^2 \frac{\partial \mathbf{u}}{\partial y} = -\frac{1}{\varepsilon}(\mathbf{v} - \mathbf{l}(\mathbf{u})) \end{aligned} \tag{47}$$

with initial conditions

$$\mathbf{u}(x, y, 0) = \mathbf{u}_0(x, y), \quad \mathbf{v}(x, y, 0) = \mathbf{f}(\mathbf{u}_0(x, y)), \quad \mathbf{w}(x, y, 0) = \mathbf{l}(\mathbf{u}_0(x, y)) \tag{48}$$

here $\mathbf{A}^2 = \mathrm{diag}(a_1^2, \ldots, a_n^2)$ and $\mathbf{B}^2 = \mathrm{diag}(b_1^2, \ldots, b_n^2)$ are diagonal matrices. The elements of $\mathbf{A}$ and $\mathbf{B}$ are to be chosen according to the sub-characteristic condition [19–21] as follows:

$$\frac{|\lambda_i|}{a_i} + \frac{|\mu_i|}{b_i} \leqslant 1, \quad i = 1, 2, \ldots, m \tag{49}$$

Here, λ_i, μ_i are the characteristic values of $\mathbf{f}'(\mathbf{u}), \mathbf{l}'(\mathbf{u})$, respectively, and a_i, $b_i > 0$. Suppose the spatial grid points are located at $(x_{i+1/2}, y_{j+1/2})$, and the grid spacings in x and y directions are $h_i^x = x_{i+1/2} - x_{i-1/2}$ and $h_j^y = y_{j+1/2} - y_{j-1/2}$, respectively.

We use the notation $\omega_{i\pm1/2,j}(t) = \omega(x_{i\pm1/2}, y_j, t)$ and $\omega_{i,j\pm1/2}(t) = \omega(x, y_{j\pm1/2}, t)$ and $\omega_{i,j} = \frac{1}{h_i^x h_j^y} \int_{x_{i-1/2}}^{x_{i-1/2}} \int_{y_{j-1/2}}^{y_{j-1/2}} \omega(x, y, t)\, \mathrm{d}x\, \mathrm{d}y$, to denote the point values and approximate cell averages of ω at $(x_{i\pm1/2}, y_j, t)$, $(x_i, y_{j\pm1/2}, t)$. We define the finite differences

$$D_x \omega_{i,j} = \frac{\omega_{i+1/2,j} - \omega_{i-1/2,j}}{h_i^x}$$

and

$$D_y \omega_{i,j} = \frac{\omega_{i,j+1/2} - \omega_{i,j-1/2}}{h_j^y}$$

then the semi-discrete approximation of (47) is given by

$$\begin{aligned} &\frac{\mathrm{d}\mathbf{u_{i,j}}}{\mathrm{d}t} + D_x \mathbf{v_{i,j}} + D_y \mathbf{w_{i,j}} = 0 \\ &\frac{\mathrm{d}\mathbf{v_{i,j}}}{\mathrm{d}t} + \mathbf{A}^2 D_x \mathbf{u_{i,j}} = -\frac{1}{\varepsilon}(\mathbf{v_{i,j}} - \mathbf{f}(\mathbf{u_{i,j}})) \\ &\frac{\mathrm{d}\mathbf{w_{i,j}}}{\mathrm{d}t} + \mathbf{B}^2 D_x \mathbf{u_{i,j}} = -\frac{1}{\varepsilon}(\mathbf{w_{i,j}} - \mathbf{l}(\mathbf{u_{i,j}})) \end{aligned} \tag{50}$$

Copyright © 2007 John Wiley & Sons, Ltd.

DOI: 10.1002/fld

We now extend the numerical flux function (18) for linear characteristic variables $\mathbf{v} \pm \mathbf{Au}$ and $\mathbf{w} \pm \mathbf{Bu}$ in x and y direction, respectively. We have the following numerical flux for the pth component of characteristic variables

$$u_{i+1/2,j} = \frac{1}{2}(u_{i+1,j} + u_{i,j}) - \frac{1}{2a_p}(v_{i+1,j} - v_{i,j}) + \frac{1}{4a_p}(h_i^x \sigma_{i,j}^{x,+} + h_{i+1}^x \sigma_{i+1,j}^{x,-})$$
$$v_{i+1/2,j} = \frac{1}{2}(v_{i+1,j} + v_{i,j}) - \frac{a_p}{2}(u_{i+1,j} - u_{i,j}) + \frac{1}{4}(h_i^x \sigma_{i,j}^{x,+} - h_{i+1}^x \sigma_{i+1,j}^{x,-}) \tag{51}$$

$$u_{i,j+1/2} = \frac{1}{2}(u_{i,j+1} + u_{i,j}) - \frac{1}{2b_p}(w_{i,j+1} - w_{i,j}) + \frac{1}{4b_p}(h_j^y \sigma_{i,j}^{y,+} + h_{j+1}^y \sigma_{i,j+1}^{y,-})$$
$$w_{i,j+1/2} = \frac{1}{2}(w_{i+1,j} + w_{i,j}) - \frac{b_p}{2}(u_{i,j+1} - u_{i,j}) + \frac{1}{4}(h_j^y \sigma_{i,j}^{y,+} - h_{j+1}^y \sigma_{i,j+1}^{y,-}) \tag{52}$$

where the slope limiters are defined as

$$\sigma_{i,j}^{x,\pm} = \frac{1}{h_i^x}\Delta_{\mp}^x(v_{i,j} \pm a_p u_{i,j})\phi(\theta_{i,j}^{x,\pm})$$
$$\theta_{i,j}^{x,\pm} = \frac{\Delta_{\mp}^x(v_{i-1,j} \pm a_p u_{i-1,j})}{\Delta_{\mp}^x(v_{i,j} \pm a_p u_{i,j})} \tag{53}$$

$$\sigma_{i,j}^{y,\pm} = \frac{1}{h_j^y}\Delta_{\mp}^y(w_{i,j} \pm b_p u_{i,j})\phi(\theta_{i,j}^{y,\pm})$$
$$\theta_{i,j}^{y,\pm} = \frac{\Delta_{\mp}^y(w_{i,j-1} \pm b_p u_{i,j-1})}{\Delta_{\mp}^y(w_{i,j} \pm b_p u_{i,j})} \tag{54}$$

with $\Delta_+^x u_{i,j} = u_{i+1,j} - u_{i,j} = \Delta_-^x u_{i+1,j}$ and $\Delta_+^y u_{i,j} = u_{i,j+1} - u_{i,j} = \Delta_-^y u_{i,j+1}$. For integration in time, the second-order IMEX Runge–Kutta method given in Table I is used. It yields second-order relaxation scheme for relaxation system (47). The relaxed system can be obtained by passing $\varepsilon \to 0$ as follows:

$$\frac{\partial}{\partial t}\mathbf{u} + \frac{\partial}{\partial x}\mathbf{f}(\mathbf{u}) + \frac{\partial}{\partial y}\mathbf{l}(\mathbf{u}) = 0 \tag{55}$$

Its corresponding relaxed scheme is given by semi-discrete conservative approximation

$$\frac{\partial}{\partial t}\mathbf{u}_{i,j} + \frac{1}{h_i^x}(\mathbf{F}_{i+1/2,j} - \mathbf{F}_{i-1/2,j}) + \frac{1}{h_j^y}(\mathbf{L}_{i,j+1/2} - \mathbf{L}_{i,j-1/2}) = 0 \tag{56}$$

Copyright © 2007 John Wiley & Sons, Ltd.

DOI: 10.1002/fld

where the pth components of the numerical fluxes are given by

$$\begin{aligned} F^p_{i+1/2,j} &= v_{i+1/2,j}|_{v=f^p(\mathbf{u})} \\ &= \frac{1}{2}(f^p(\mathbf{u}_{i+1,j}) + f^p(\mathbf{u}_{i,j})) - \frac{a_p}{2}(u_{i+1,j} - u_{i,j}) \\ &\quad + \frac{1}{4}(h^x_i \sigma^{x,+}_{i,j} - h^x_{i+1}\sigma^{x,-}_{i+1,j})\Big|_{v=f^p(\mathbf{u})} \\ L^p_{i,j+1/2} &= w_{i,j+1/2}|_{w=l^p(\mathbf{u})} \\ &= \frac{1}{2}(l^p(\mathbf{u}_{i,j+1}) + l^p(\mathbf{u}_{i,j})) - \frac{b_p}{2}(u_{i,j+1} - u_{i,j}) \\ &\quad + \frac{1}{4}(h^y_j \sigma^{y,+}_{i,j} - h^y_{j+1}\sigma^{y,-}_{i,j+1})\Big|_{w=l^p(\mathbf{u})} \end{aligned} \tag{57}$$

with the slope limiters

$$\begin{aligned} \sigma^{x,\pm}_{i,j}|_{v=f^p(\mathbf{u})} &= \frac{1}{h^x_i}\Delta^x_{\mp}(f^p(\mathbf{u}_{i,j}) \pm a_p u_{i,j})\phi(\theta^{x,\pm}_{i,j}) \\ \theta^{x,\pm}_{i,j} &= \frac{\Delta^x_{\mp}(f^p(\mathbf{u}_{i-1,j}) \pm a_p u_{i-1,j})}{\Delta^x_{\mp}(f^p(\mathbf{u}_{i,j}) \pm a_p u_{i,j})} \\ \sigma^{y,\pm}_{i,j}|_{w=l^p(\mathbf{u})} &= \frac{1}{h^y_j}\Delta^y_{\mp}(l^p(\mathbf{u}_{i,j}) \pm b_p u_{i,j})\phi(\theta^{y,\pm}_{i,j}) \\ \theta^{y,\pm}_{i,j} &= \frac{\Delta^y_{\mp}(l^p(\mathbf{u}_{i,j-1}) \pm b_p u_{i,j-1})}{\Delta^x_{\mp}(l^p(\mathbf{u}_{i,j}) \pm b_p u_{i,j})} \end{aligned} \tag{58}$$

Note that, u, v, w, f^p, l^p, F, L are the pth components of $\mathbf{u}, \mathbf{v}, \mathbf{w}, \mathbf{f}, \mathbf{l}, \mathbf{F}, \mathbf{L}$, respectively, and the limiter function ϕ should satisfy the condition $0 \leqslant \phi(\theta) \leqslant 1$. Again, for time discretization we use IMEX Runge–Kutta method given in Table I. Also note that the formulation of 2-D relaxation system is similar to the 1-D system, hence one can formulate the n-dimensional relaxation system for $n > 2$ and its corresponding relaxation scheme in a similar way. In fact, the numerical implementation based on dimension by dimension is not much harder than 1-D problems.

Remarks

1. The proposed relaxation scheme is much efficient as compared to the other TVD schemes and the relaxation scheme presented in [12]. It is because one can avoid computing the flux limiter function ϕ at each grid point of whole computational domain by fixing the constant value of $\phi \in [0, 1]$.
2. To prevent the initial as well as boundary layer, initial conditions and boundary conditions of the equilibrium system are applied (see (2)).
3. One can have different choices for ε and matrices $\mathbf{A}, \mathbf{B}$. Some choices are given in [12].

Copyright © 2007 John Wiley & Sons, Ltd.

DOI: 10.1002/fld

4. Note that, for small ε, numerical solution obtained by the relaxed scheme is the same as that of the relaxation scheme. One can directly implement the relaxed scheme for solving conservation laws.
5. Introduction of second-order integration of the flux neither introduces nonlinear equation nor the nonlinear source terms. In fact, at each stage of the second-order IMEX Runge–Kutta integration, the values of **u** are computed explicitly and used in the computation of the flux **v**.

6. NUMERICAL RESULTS

6.1. 1-D test results

In all our numerical examples, we have chosen different values of limiter function ϕ. In some test cases we have compared the numerical result for $\phi = 1.0$ with some second-order accurate methods in terms of Ł$^\infty$ error norm.

We do not compare the obtained results with any preexisting high-resolution relaxation methods (of [12, 22]) or high-resolution methods (of [12, 14, 18, 23–25]), as they *fail* to remain TVD for any *constant non-zero* value of ϕ. Also for $\phi = 1.0$, though, conceptually they become second-order accurate but at the same time become too oscillatory. In some test cases, (e.g. Lax tube problem), even oscillatory computational results could not be obtained at constant $\phi = 1.0$ using other TVD schemes, but proposed scheme gives acceptable results. We used $\varepsilon = 10^{-8}$ for all our computations as suggested in [12].

6.1.1. Pure convection problem. One of the simplest model problems is the 1-D convection at constant velocity α, given by

$$u_t + \alpha u_x = 0, \quad x \in [0, 2\pi], \quad \alpha = 1 \tag{59}$$

with initial condition $u(x, 0) = 0.5 + \sin(x)$ and periodic boundary conditions. The analytical solution of the above equation is $u = f(x - \alpha t)$, where $f(x)$ is the initial distribution of u. The solution describes a wave propagating in the positive x-direction with velocity α without losing its initial shape. The associated relaxation system for (59) is constructed as in (2). We choose $a^2 = \alpha = 1$ as it satisfies sub-characteristic condition (3), [26]. We take $\varepsilon = 10^{-8}$, $C = 0.3$ in our computations. In Tables II and III, we display the L^∞ and L^2-error norms, respectively, and compared with the errors in Lax–Friedrich's (LxF) scheme at $t = 1.0$ for various choices of ϕ. Errors are not shown for the relaxed schemes as they are similar to the relaxation schemes. We also display in Figure 2, the comparison of the exact solution and computed solution for LxF scheme and resulting relaxation scheme for $\phi = 1.0$ using space step $\Delta x = 0.0785$ at time $t = 1.0$. Graph shows that proposed scheme do not introduce spurious oscillations for $\phi = 1.0$.

6.1.2. Inviscid Burger equation. We take inviscid Burger equation along with the sinusoidal initial condition as our second test problem as follows:

$$u_t + \left(\frac{u^2}{2}\right)_x = 0 \tag{60}$$

Copyright © 2007 John Wiley & Sons, Ltd.

DOI: 10.1002/fld

Table II. Comparison of errors in L^∞-norm with I order Lax–Friedrich's scheme.

L^∞ error at time $t = 1.0$			
Δx	LxF	$\phi = \max[0, \min(1, \theta)]$	$\phi = 1.0$
0.628	0.529475	0.211099	0.159597
0.314	0.350763	0.107643	0.124809
0.157	0.206233	0.088605	0.074711
0.0785	0.112955	0.044628	0.042824

Table III. Comparison of errors in L^2-norm with I order Lax–Friedrich's scheme.

L^2 error at time $t = 1.0$			
Δx	LxF	$\phi = \max[0, \min(1, \theta)]$	$\phi = 1.0$
0.628	0.305142	0.098724	0.081111
0.314	0.207765	0.066032	0.081007
0.157	0.129483	0.040698	0.040213
0.0785	0.071350	0.024388	0.023419

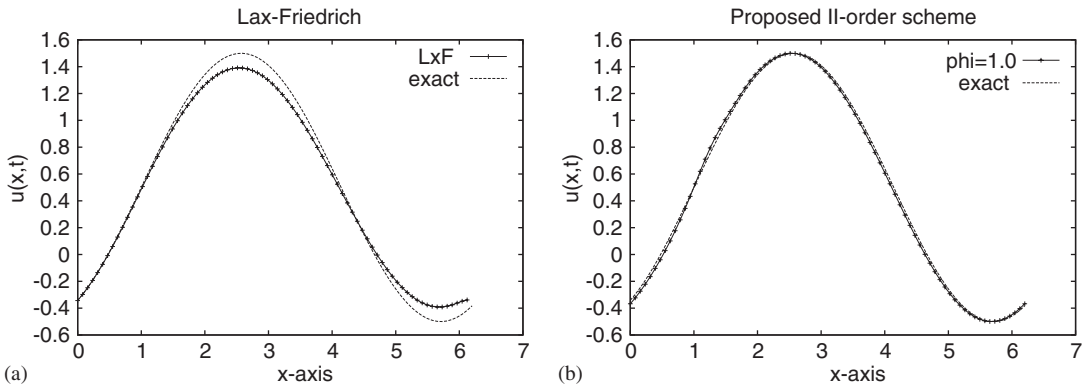

Figure 2. 1-D Pure convection problem: (a) Lax–Friedrich's and (b) proposed scheme for $\phi = 1.0$.

with the initial condition $u(x, 0) = -\tau \sin(x)$ and periodic boundary conditions. It is a consequence of nonlinearity of (60) that the (non-trivial) solution beginning from smooth initial conditions will eventually develop a finite-time derivative singularity. In 1964, Platzman produced an exact Fourier sine series solution to (60), given by

$$u(x, t) = -2 \sum_{n=1}^{\infty} \frac{J_n(\tau n t)}{n t} \sin(nx) \tag{61}$$

Copyright © 2007 John Wiley & Sons, Ltd.

DOI: 10.1002/fld

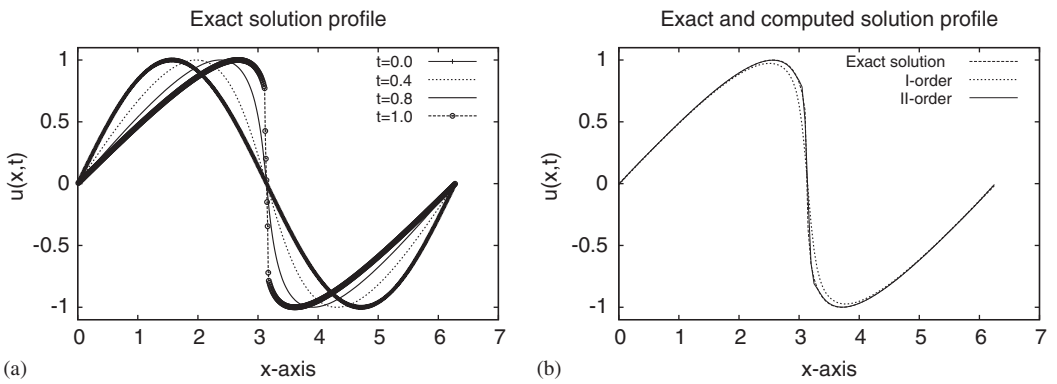

Figure 3. Solution of 1-D Burger equation: (a) Fourier series solution and (b) comparison of numerical solutions at time $t = 1.0$.

where J_n is the Bessel function. Note that, in the $t \to 0^+$ limit, only the term $n = 1$ is non-zero and the initial condition $u(x, 0) = -\tau \sin(x)$ is satisfied. This Fourier representation is valid prior to wave breaking [27]. Recall that the unique entropy solution of (60) is smooth up to critical time $t = 1$. In Figure 3(a), we give the solution obtained by Fourier series representation (61) for $\tau = -1$ and the comparison of exact solution with computed solution for $\phi = 0.0$ and 1.0 at time $t = 1.0$ is shown in Figure 3(b). For computation we set $\Delta x = 0.05$, CFL number $C = 0.5$ and $a^2 = 1.23$ according to sub-characteristic condition (3), [26].

6.2. *Inviscid Euler equations*

Here, we consider the 1-D Euler system of gas dynamics given by

$$\frac{\partial}{\partial t}\begin{pmatrix} \rho \\ \rho v \\ E \end{pmatrix} + \frac{\partial}{\partial x}\begin{pmatrix} \rho v \\ \rho v^2 + p \\ v(E+p) \end{pmatrix} = 0 \tag{62}$$

which can be considered as

$$\frac{\partial}{\partial t}\mathbf{u} + \frac{\partial}{\partial x}\mathbf{f}(\mathbf{u}) = 0 \tag{63}$$

where $\mathbf{u} = (\rho, \rho v, E)^{\mathrm{T}}$, $\mathbf{f}(\mathbf{u}) = (\rho v, \rho v^2 + p, v(E+p))^{\mathrm{T}}$, and ρ, v, ρv, E, p are density, velocity, momentum, energy and pressure, respectively. To solve Equation (62), the equation of the state $p = (\gamma - 1)(E - \frac{1}{2}\rho v^2)$ is required, where $\gamma = 1.4$ is the specific heat. One can construct a relaxation system for (62) as in (2), where $\mathbf{A^2} = \mathrm{diag}(a_1^2, a_2^2, a_3^2)$. We define the CFL number as in (27).

6.2.1. Sod tube test. The first test is the typical Sod tube problem [28]. Its solution consists of a left rarefaction, a contact and a right shock. This test is useful in assessing the entropy satisfaction

Copyright © 2007 John Wiley & Sons, Ltd.

DOI: 10.1002/fld

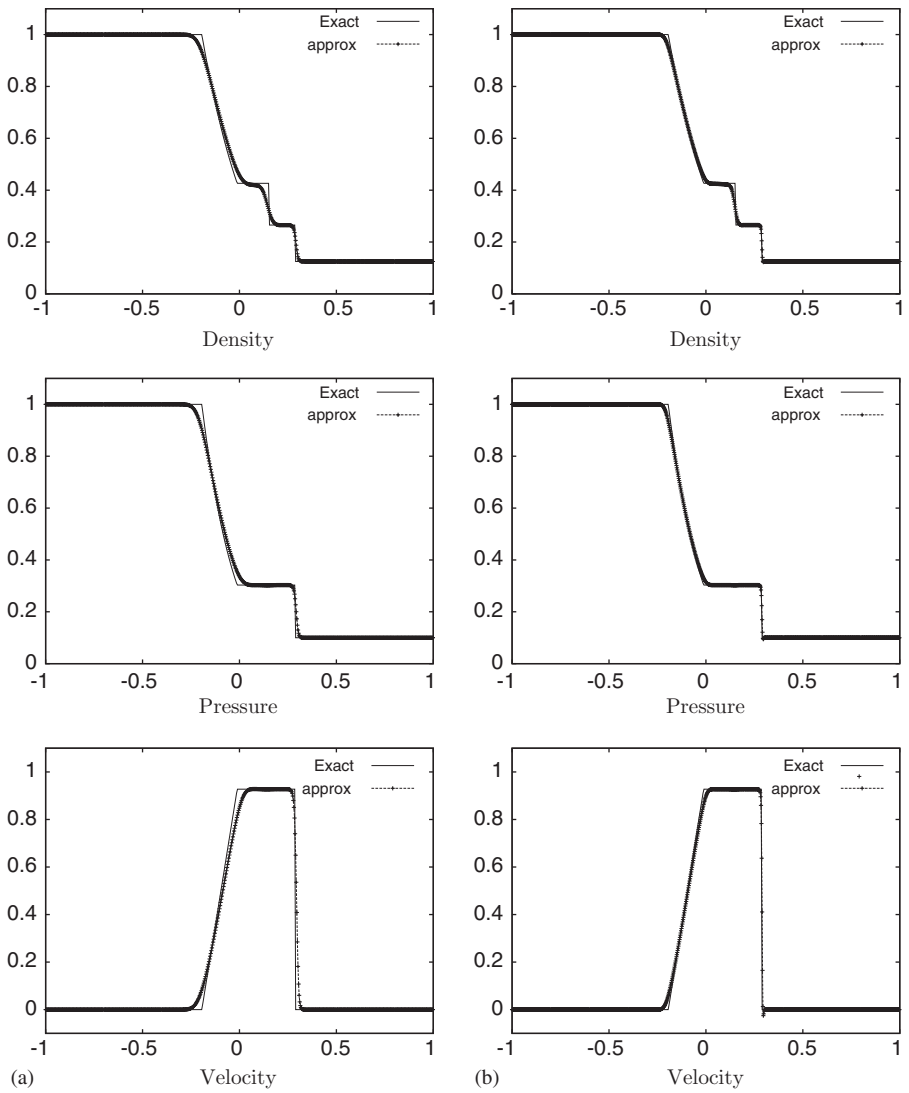

Figure 4. Solution profile of Sod shock tube: (a) $\phi = 0.0$ and (b) $\phi = 0.5$.

property of any numerical method [2]. It is formulated by (62) with the initial condition given by

$$u(x, y, 0) = \begin{cases} (1, 0, 2.5)^{\mathrm{T}} & \text{if } -1.0 \leqslant x, y \leqslant 0.0 \\ (0.125, 0, 0.25)^{\mathrm{T}} & \text{if } 0.0 \leqslant x \leqslant 1.0 \end{cases} \tag{64}$$

For computation, we choose $a_1^2 = 1, a_2^2 = 1.68, a_3^2 = 5.045$, according to sub-characteristic condition (3), as suggested in [12] and $\Delta x = 0.002,\ C = 0.4$.

Figure 4 shows the graphs obtained at time $t = 0.245$ for the flux limiters $\phi = 0.0$ and 0.5, respectively. Graphs show that underlying scheme is able to capture the right shock, rarefaction

Copyright © 2007 John Wiley & Sons, Ltd.

DOI: 10.1002/fld

Table IV. Comparison of errors in L^∞-norm with Lax–Wendroff scheme.

Space step	Relaxation scheme for $\phi = 1.0$ L^∞-error			Lax–Wendroff L^∞-error		
Δx	Density	Pressure	Velocity	Density	Pressure	Velocity
0.05	1.40×10^{-1}	1.93×10^{-1}	4.20×10^{-1}	1.950	1.850	1.027
0.01	7.74×10^{-2}	1.10×10^{-1}	5.8×10^{-1}	1.990	1.970	1.107
0.005	7.12×10^{-2}	9.83×10^{-2}	5.30×10^{-1}	1.995	1.985	1.137
0.001	8.45×10^{-2}	6.31×10^{-2}	3.96×10^{-1}	1.999	1.997	1.138

and resolve the contact discontinuity. We compare the results in terms of Ł$^\infty$-error norm of proposed second-order scheme corresponding to $\phi = 1.0$, $\Delta x = 0.005$ with Lax–Wendroff second-order scheme in Table IV, in order to show that the resulting scheme is able to suppress oscillations. Table IV shows that the errors in the proposed scheme are less than the second-order accurate Lax–Wendroff scheme.

We do not compare numerical results obtained using the proposed scheme with other TVD schemes (e.g. [12, 14, 18, 23–25]) as they fail to be TVD for any non-zero fixed value of limiter function ϕ. In fact for $\phi = 1.0$, though theoretically they become second-order accurate but also become unstable which leads to too oscillatory computational results for Sod tube problem.

6.2.2. Lax-tube test. The second shock tube problem is Lax-tube problem. It is formulated by (62) with the initial condition given by

$$u(x, y, 0) = \begin{cases} (0.445, 0.311, 8.928)^{\mathrm{T}} & \text{if } 0.0 \leqslant x, y \leqslant 0.5 \\ (0.5, 0, 0.4275)^{\mathrm{T}} & \text{if } 0.5 \leqslant x \leqslant 1.0 \end{cases} \tag{65}$$

According to sub-characteristic condition (3), we take $a_1^2 = 2.4025$, $a_2^2 = 11$, $a_3^2 = 22.2056$, as suggested in [12] and $\Delta x = 0.002$, $C = 0.4$ for computation of this problem. Figure 5 shows the graphs obtained at time $t = 0.16$ for the flux limiters $\phi = 0.0$ and 0.5, respectively. In case of Lax-tube, small oscillation occurs in the computed solution, using underlying scheme, for higher constant values of ϕ. Again, we do not compare underlying second-order scheme corresponding to $\phi = 1.0$ with Lax–Wendroff or any other TVD scheme (e.g. [12, 14, 18, 23–25]) as they end up with no computational solution for Lax-tube problem for $\phi = 1.0$ because of the said reason. Graphs show that the scheme is able to capture the contact, rarefaction and right shock.

6.3. 2-D numerical tests

6.3.1. 2-D pure convection equation. We take the 2-D pure convection equation as first 2-D test example, given by

$$u_t + u_x + u_y = 0, \quad (x, y) \in [0, 4] \times [0, 4] \tag{66}$$

with initial condition

$$u(x, y, 0) = \begin{cases} \sin^2(\pi x) \sin^2(\pi y) & \text{if } 0.0 \leqslant x, y \leqslant 1.0 \\ 0 & \text{else} \end{cases} \tag{67}$$

Copyright © 2007 John Wiley & Sons, Ltd.

DOI: 10.1002/fld

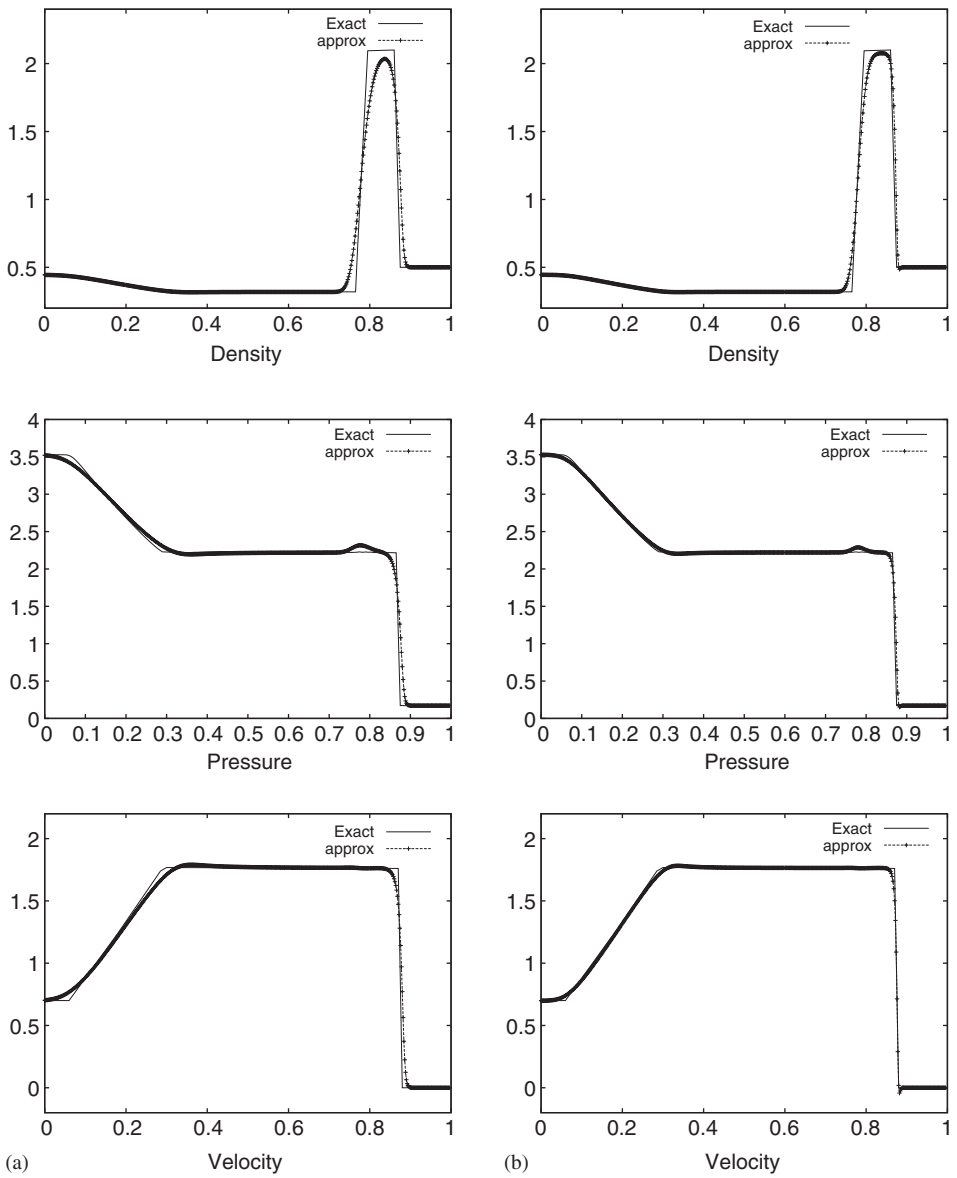

Figure 5. Solution profile of Lax shock tube for: (a) $\phi = 0.0$ and (b) $\phi = 0.5$.

The solution surface convects in the x–y plane without losing its initial shape. In Figure 6, both surface and cross-sectional plots of the solution profile for constant values $\phi = 0.0$, 1.0 and the min-mod limiter are given. We use the parameters $a = 1.0, b = 1.0$ as in [26] and $\varepsilon = 10^{-8}$.

Copyright © 2007 John Wiley & Sons, Ltd.

DOI: 10.1002/fld

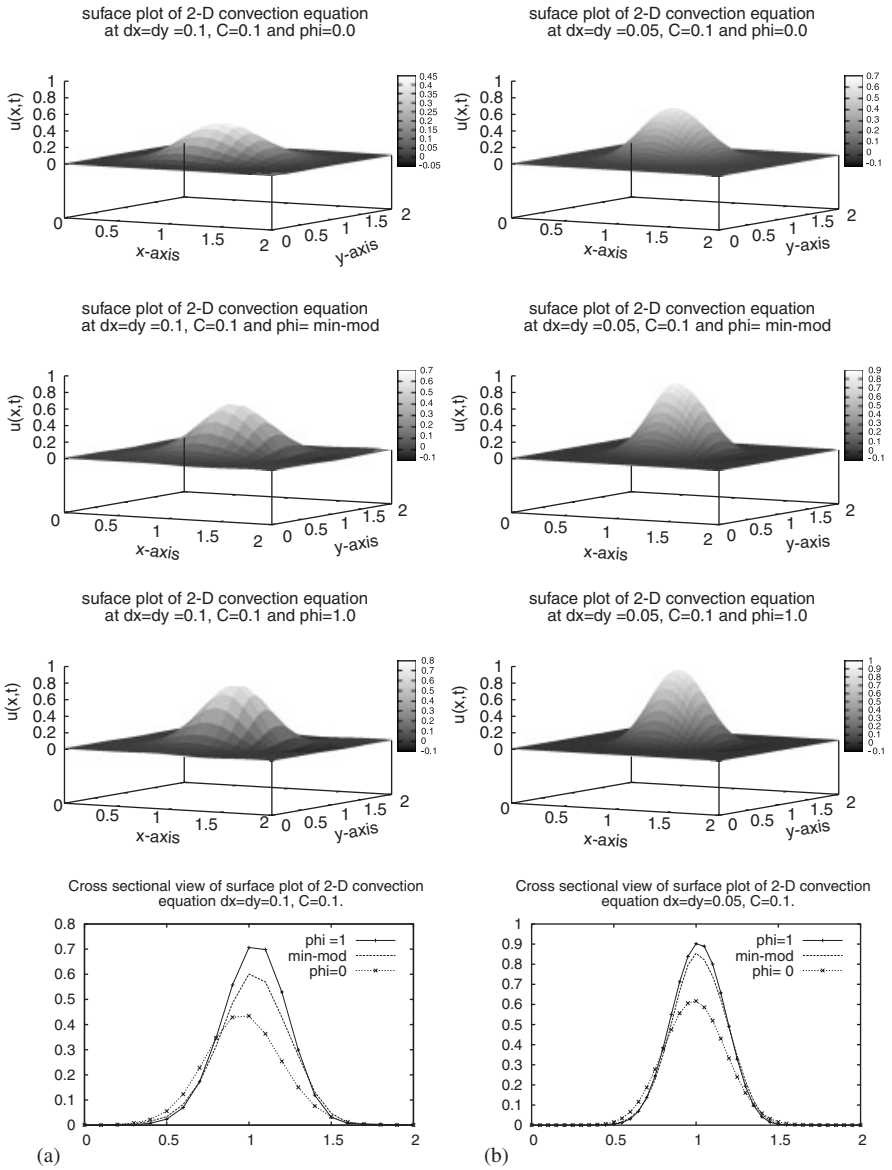

Figure 6. Solution surface of 2-D pure convection equation: (a) $\Delta x = \Delta y = 0.1$ and (b) $\Delta x = \Delta y = 0.05$.

For Figure 6(a), $\Delta x = \Delta y = 0.1$, $C = 0.1$ and for Figure 6(b), $\Delta x = \Delta y = 0.05$, $C = 0.1$ parameters are taken. These plots show that the solution profile advects in positive x–y direction without losing its initial shape. The scheme does not introduce any spurious oscillations for $\phi = 1.0$.

Copyright © 2007 John Wiley & Sons, Ltd.

DOI: 10.1002/fld

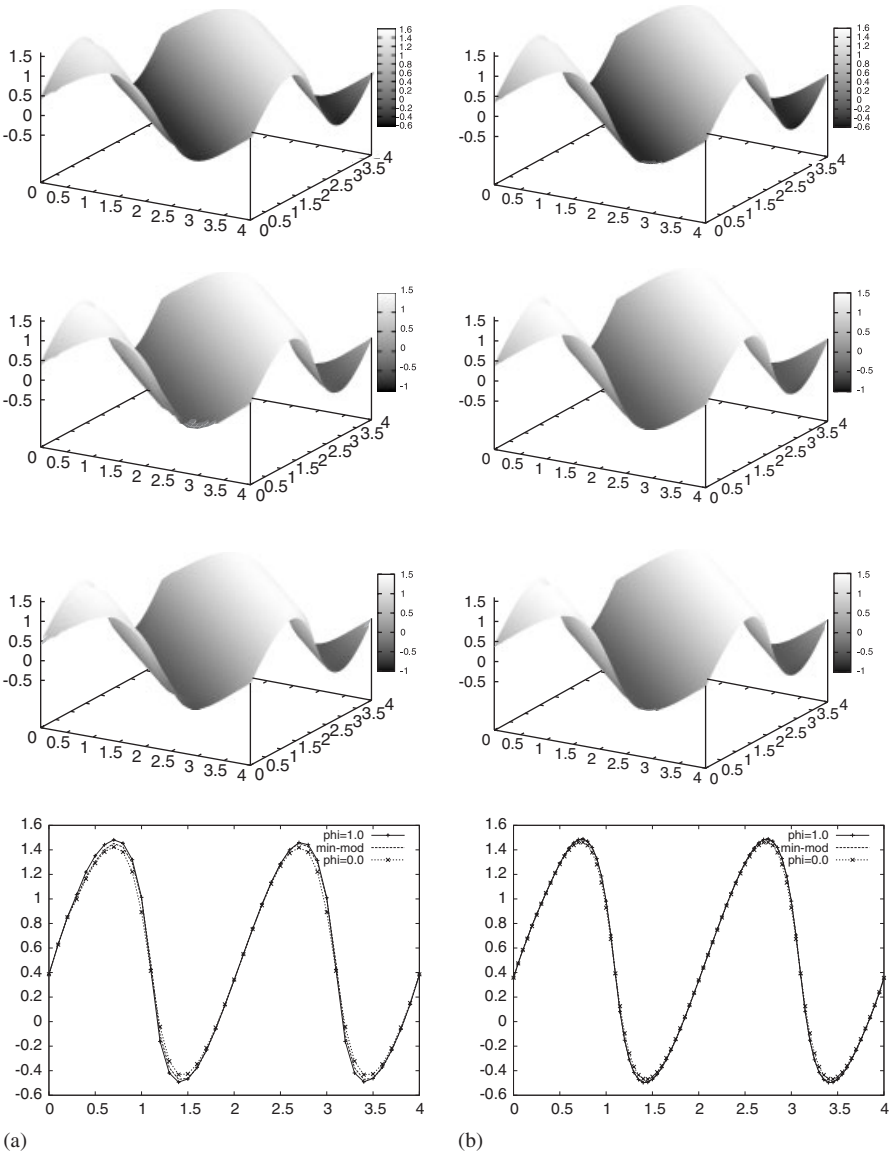

Figure 7. Numerical results of 2-D Burger's equation: (a) $\Delta x = \Delta y = 0.1$ and (b) $\Delta x = \Delta y = 0.05$.

6.3.2. 2-D inviscid Burger equation. The second 2-D test case is 2-D inviscid Burger equation, given by

$$\frac{\partial}{\partial t}u + \frac{\partial}{\partial x}\left(\frac{u^2}{2}\right) + \frac{\partial}{\partial y}\left(\frac{u^2}{2}\right) = 0, \quad (x, y) \in [0, 4] \times [0, 4] \tag{68}$$

Copyright © 2007 John Wiley & Sons, Ltd.

DOI: 10.1002/fld

with initial condition $u(x, y, 0) = 0.5 + \sin(\pi(x+y)/2)$ and a 4-periodic boundary condition. When $t = 1.0/\pi$, the solution remains smooth. We give the numerical results obtained at time $t = 1.0/\pi$ for constant values of the limiter $\phi = 0.0$, 1.0 and the min-mod limiter. We use $a = b = 1.5$ satisfying the sub-characteristic condition, $C = 0.1$, $\varepsilon = 10^{-8}$ and two different mesh sizes $\Delta x = \Delta y = 0.1$ and $\Delta x = \Delta y = 0.05$ for our computation. In Figure 7, both surface and cross-sectional plots of the solution profile are given. These plots show that, the scheme does not introduce spurious oscillations even for the constant value of the limiter, $\phi = 1.0$.

Remark 1

The improvement in the obtained numerical results using $\phi = 1.0$ over $\phi = 0.0$ can be seen from the cross-sectional plots of 2-D problems. For 2-D Burger equation this improvement is not too prominent but for 2-D convection problem, improvement is significant though there is a loss in the maxima and minima of the solution profile. It shows a slight dissipative nature of the resulting scheme, for $\phi = 1.0$. Also note that in both the 2-D test problems, the resulting scheme, corresponding to $\phi = 1.0$, does not introduce spurious oscillations, which shows that, the scheme remains TVD for 2-D case. This observation is well supported by Goodman and Leveque's [29] and Tang' work [30], that in 2-D case TVD schemes can not be second-order accurate (see also [19–21]).

Remark 2

Note that the proposed scheme has an advantage over the other TVD schemes, that for any fixed non-zero value of flux limiter function it efficiently works and gives TVD results, while other high-resolution TVD schemes fail to remain TVD for any non-zero fixed value of the limiter function and gives disastrous results. The class of schemes such as ENO [16, 31] and WENO [23], though, can give very high accuracy without introducing oscillations, but at the same time they are computationally costly as compared to the proposed scheme.

7. CONCLUSION

Based on the local relaxation approximation, a class of simple and general numerical schemes is presented for the system of conservation laws. The computational cost of the presented scheme is much less than other schemes of this kind as the proposed scheme works nicely even for the constant values of the limiter function and remains TVD. It uses neither the Riemann solver spatially nor the nonlinear systems of algebraic equations solvers temporally, yet can achieve higher accuracy and converges to the correct weak solution. The second-order relaxed scheme for 1-D scalar equation is shown to be TVD. Numerical results for various test problems are given and compared. Numerical results show that for the test problems with smooth initial conditions, the proposed scheme can give second-order accuracy without introducing oscillations. In fact, one can use the min-mod limiter for such cases to obtain good results. For complex problems with discontinuous initial condition, it gives good results for smaller fixed value of limiter function. Although resulting second-order accurate scheme may give some oscillations for such problems but, they are much smaller than other second-order accurate schemes. This shows that the scheme is able to suppress the oscillations as expected. Good accuracy without spurious oscillations may be obtained by defining new flux limiters as functions of θ, which should satisfy the TVD condition $\phi \in [0, 1]$ [32].

Copyright © 2007 John Wiley & Sons, Ltd.

DOI: 10.1002/fld

REFERENCES

1. Laney CB. *Computational Gas Dynamics* (1st edn). Cambridge University Press: Cambridge, 1998.
2. Toro EF. *Riemann Solvers and Numerical Methods for Fluid Dynamics*, *A Practical Introduction* (2nd edn). Springer: Berlin, 1999.
3. Thomas JW. *Numerical Partial Differential Equations*, *Conservation Laws and Elliptic Equations*. Text in Applied Mathematics, vol. 33. Springer: Berlin, 1999.
4. Ewing RE, Wang H. A summary of numerical methods for time-dependent advection-dominated partial differential equations. *Journal of Computational and Applied Mathematics* 2001; **128**:423–445.
5. Levaque RJ. *Numerical Methods for Conservation Laws Lectures in Mathematics*. Birkhauser: ETH Zurich, 1999.
6. Wang Y, Hutter K. Comparisons of numerical methods with respect to convectively dominated problems. *International Journal for Numerical Methods in Fluids* 2001; **37**:721–745.
7. Fletcher CAJ. *Computational Techniques for Fluid Dynamics*, *Part I*. Springer Series in Computational Physics. Springer: Berlin, 1988.
8. Harten A. High resolution schemes for conservation law. *Journal of Computational Physics* 1983; **49**:357–393.
9. Osher S, Chakravarthy S. High resolution schemes and entropy condition. *SIAM Journal on Numerical Analysis* 1984; **21**:955–984.
10. Kadalbajoo MK, Ritesh Kumar. A high resolution total variation diminishing scheme for hyperbolic conservation law and related problems. *Applied Mathematics and Computation* 2006; **175**:1556–1573.
11. Kadalbajoo MK, Ritesh Kumar. High resolution scheme for linear hyperbolic systems. *SIAM Conference on Analysis of Partial Differential Equations*, Boston, Massachusetts, 10–12 July 2006.
12. Jin S, Xin Z. The relaxation schemes for systems of hyperbolic conservation laws in arbitrary space dimension. *Communications on Pure and Applied Mathematics* 1995; **48**:235–276.
13. Liu TP. Hyperbolic conservation laws with relaxation. *Communications in Mathematical Physics* 1987; **108**: 153–175.
14. van Leer B. Towards the ultimate conservative difference scheme V. A second order sequel to Godunov's method. *Journal of Computational Physics* 1979; **32**:101–136.
15. Jin S. Runge–Kutta methods for hyperbolic systems with relaxation terms. *Journal of Computational Physics* 1995; **122**:51–67.
16. Shu CW. An overview on high order numerical methods for convection dominated PDEs. In *Hyperbolic Problems*: *Theory*, *Numerics*, *Applications*, Hou TY, Tadmor E (eds). Springer: Berlin, 2003; 79–88.
17. Gottlib S, Shu CW, Tadmor E. Strong stability-preserving high-order time discretization methods. *SIAM Review* 2000; **43**:89–112.
18. Sweby PK. High resolution schemes using flux limiters for Hyperbolic conservation Laws. *SIAM Journal on Numerical Analysis* 1984; **21**:995–1010.
19. Chalabi A. Convergence of the relaxation scheme for hyperbolic conservation laws with stiff source terms. *Mathematics of Computation* 1999; **68**:955–970.
20. Lattanzio C, Serre D. Convergence of a relaxation scheme for hyperbolic systems of conservation laws. *Numerische Mathematik* 2001; **88**:121–134.
21. Liu HL, Warnecke G. Convergence rates for relaxation schemes approximating conservation laws. *SIAM Journal on Numerical Analysis* 2000; **37**:1316–1337.
22. Aregba Driollet D, Natalini R. Discrete kinetic schemes for multidimensional conservation laws. *SIAM Journal on Numerical Analysis* 2000; **37**(6):1973–2004.
23. Kurganov A, Tadmor E. New high resolution central schemes for nonlinear conservation laws and convection diffusion equations. *Journal of Computational Physics* 2000; **160**:241–282.
24. Jonathan B, Leveque RJ. A geometric approach to high resolution schemes. *SIAM Journal on Numerical Analysis* 1988; **25**:268–284.
25. van Leer B. Towards the ultimate conservative scheme, II. Monotonicity and conservation combined in a second order scheme. *Journal of Computational Physics* 1974; **14**:361–370.
26. Banda MK, Seaid M. Higher-order relaxation schemes for hyperbolic systems of conservation laws. *Journal of Numerical Mathematics* 2005; **13**:171–196.
27. Platzman GW. An exact integral of complete spectral equations for unsteady one-dimensional flow. *Tellus* 1964; **XVI**:422–431.
28. Sod G. A survey of several finite difference scheme for systems of nonlinear hyperbolic conservation laws. *Journal of Computational Physics* 1978; **27**:159–193.

Copyright © 2007 John Wiley & Sons, Ltd.

DOI: 10.1002/fld

29. Goodman J, Leveque RJ. On the accuracy of stable scheme for 2D scalar conservation Laws. *Mathematics of Computation* 1985; **45**:15–21.
30. Tang HZ, Tang T, Wang JH. On numerical entropy inequalities for second order relaxed scheme. *Quarterly of Applied Mathematics* 2001; **59**:391–399.
31. Shu CW, Osher S. Efficient implementation of essentially non-oscillatory shock-capturing schemes. *Journal of Computational Physics* 1988; **77**:439–471.
32. Piperno S, Depeyre S. Criteria for the design of limiters yielding efficient high resolution TVD schemes. *Computers and Fluids* 1998; **27**:183–197.

Copyright © 2007 John Wiley & Sons, Ltd.

DOI: 10.1002/fld